AS5545

Dynamics and Control of Spacecraft

Project Report

based on

Feedback Control Law of Solar Sail with Variable Surface Reflectivity at Sun-Earth Collinear equilibrium points

- LorenzoNiccolai, GiovanniMengali, Alessandro A.Quarta, AndreaCaruso

---

Name : Sumanth Nethi
Roll No. : AE18B042

INDEX

1 Abstract

In this report a preliminary investigation into the possibility of using a solar sail-based spacecraft to maintain a (collinear) L1-type artificial equilibrium point in the Sun - [Earth+Moon] circular restricted three-body problem has been conducted. A control system capable of adjusting the sail lightness number and attitude was assumed, and a full-state control law was tested, with control gains selected using a linear-quadratic regulator approach. The solar sail placed at such an artificial equilibrium point is of use to us as it guarantees a continuous monitoring of solar activity and is able to give an early warning in case of catastrophic solar flares. After discussing the mathematical formulation of the full-state feedback law in detail, the report follows with numerical simulations done using Python which show that an L1-type artificial equilibrium point can be maintained with small required control torques.

2 Significance

In this project report I have explored the Solar Sail topic mentioned in class in more detail. A solar sail creates thrust without using any fuel, making it a potential alternative for mission scenarios that require constant propulsive acceleration. One such significant use of solar sail is that if we manage to place it at the L1 type artificial equilibrium point [2] in the Sun-[Earth+Moon] circular restricted three-body problem, it can ensure continuous monitoring of sun's activity. Currently, NASA's Advanced Composition Explorer (ACE) is monitoring the solar activity while tracking a Lissajous orbit around the Sun-Earth L1point, which guarantees an early warning time of about 1 hour which can be further improved by using propellantless propulsion systems like the Solar Sail. But, however such vantage points are known to be intrinsically unstable and hence a suitable control system is necessary. The work discussed in [1] provides one solution on how to stabilize an L1-type artificial equilibrium point with a solar sail by adjusting lightness number and thrust vector accordingly.

3 Introduction

From the previous section we understand the significance of using solar sails to generate collinear artificial equilibrium points (AEPs). Since such equilibrium positions are intrinsically unstable, the spacecraft must be equipped with a suitable control system. While conducting literature survey, most of the studies I came across related to AEPs with a solar sail tend to be based on simplifying assumptions, such as that of an ideal (i.e., perfectly reflecting) sail or a constant sail attitude, and does not provide any estimate of the control torques required to meet the mission requirements. This project

report presents detailed analysis of the maintenance problem of an L1-type AEP in the Sun-Earth circular restricted three-body problem (CR3BP) [3] using a solar sail with Reflectivity Control Devices (RCD)-based control systems, whose purpose is to provide required control torques and thereby modify both the sail lightness number and the sail attitude. A full-state feedback control system is developed to compensate for the dynamics instability. The performance of the control law is demonstrated via numerical simulations and the required control torques are estimated by means of Euler's equations.

4 Mathematical Formulation

Consider a solar sail based spacecraft S is moving under the gravitational forces exerted by the Sun and the [Earth+Moon] (denotes the center of mass of the Earth-Moon system). The analysis of S is carried out under the assumptions of circular restricted three-body problem (CR3BP), i.e, the spacecraft mass m_S is negligible compared to Sun's mass $m_\odot$ and [Earth+Moon] system's mass $m_\oplus$, and the other assumption is the orbital eccentricity of the primaries is neglected (i.e, they are assumed to track co-planar circular orbits around the center of mass of the system C). Let the constant distance between Sun and [Earth+Moon] be l ($l = 1au$).

We will use a Cartesian synodic reference frame $\mathcal{T}(C, \hat{i}, \hat{j}, \hat{k})$ that rotates with respect to an inertial frame with a constant angular velocity of magnitude $\omega_\oplus = \sqrt{\frac{G(m_\oplus + m_\odot)}{l^3}} = 2\pi$ rad/year (G is universal gravitational constant). l is taken as reference length, $(m_\oplus + m_\odot)$ is taken as reference mass and time t is expressed as in dimensionless units by normalizing $\omega_\oplus$ to 1. Let the dimensionless mass $\mu = \frac{m_\oplus}{(m_\oplus + m_\odot)} \simeq 3.0404 \times 10^{-6}$. And finally, $\hat{i}, \hat{j}, \hat{k}$ are all as indicated in the Figure 1.

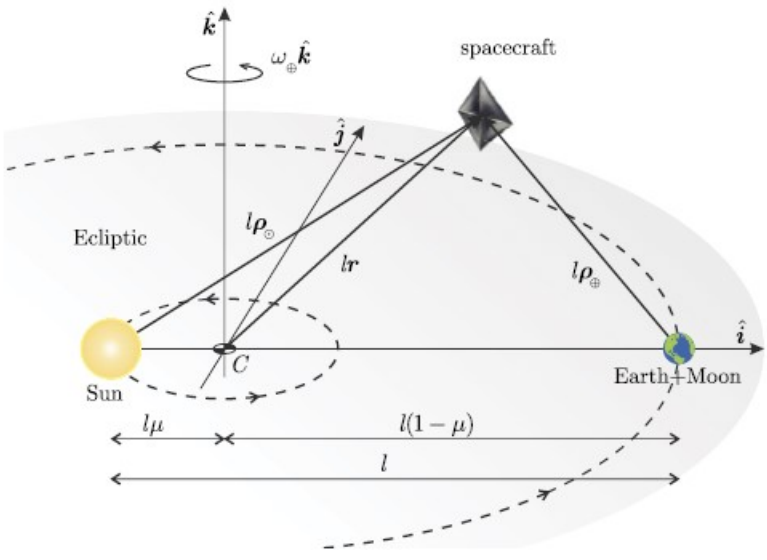

Figure 1: Sun-[Earth+Moon] framework

The angular velocity vector of rotation reference is $\hat{k}$ in dimensionless units. The motion of S is described by the following differential equation.

$$\ddot{\boldsymbol{r}} + 2\hat{\boldsymbol{k}} \times \dot{\boldsymbol{r}} + \hat{\boldsymbol{k}} \times (\hat{\boldsymbol{k}} \times \boldsymbol{r}) + \frac{1-\mu}{\rho_{\odot}^3}\boldsymbol{\rho}_{\odot} + \frac{\mu}{\rho_{\oplus}^3}\boldsymbol{\rho}_{\oplus} = \boldsymbol{a} \tag{1}$$

In the above equation $\boldsymbol{a}$ denotes the dimensionless propulsive acceleration vector provided by the solar sail. $\boldsymbol{r}, \boldsymbol{\rho}_{\odot}, \boldsymbol{\rho}_{\oplus}$ are the dimensionless position vectors of S with respect to C, the Sun and the [Earth+Moon] respectively.
From the Figure 1, using geometry, the vectors can be expressed as follows:

$$\begin{aligned} \boldsymbol{r} &= \boldsymbol{\rho}_{\odot} - \mu\hat{\boldsymbol{i}} \\ \boldsymbol{\rho}_{\oplus} &= \boldsymbol{r} - (1-\mu)\hat{\boldsymbol{i}} = \boldsymbol{\rho}_{\odot} - \hat{\boldsymbol{i}} \end{aligned} \tag{2}$$

Substituting Eq(2) in Eq(1),

$$\ddot{\boldsymbol{\rho}}_{\odot} + 2\hat{\boldsymbol{k}} \times \dot{\boldsymbol{\rho}}_{\odot} + \hat{\boldsymbol{k}} \times \left[\hat{\boldsymbol{k}} \times (\boldsymbol{\rho}_{\odot} - \mu\hat{\boldsymbol{i}})\right] + \frac{1-\mu}{\rho_{\odot}^3}\boldsymbol{\rho}_{\odot} + \frac{\mu}{\left\|\boldsymbol{\rho}_{\odot} - \hat{\boldsymbol{i}}\right\|^3}(\boldsymbol{\rho}_{\odot} - \hat{\boldsymbol{i}}) = \boldsymbol{a} \tag{3}$$

From the above equation it is evident that the spacecraft dynamics can be analysed if we have the propulsive acceleration vector $\boldsymbol{a}$. $\boldsymbol{a}$ can be described by a suitable thrust model.

4.1 Solar sail thrust model

Optical force model is used in the following analysis. It effectively takes into account the optical properties of the sail film. The model presents a good compromise between simplicity and accuracy. It is also assumes that the solar sail attitude is known at each time instant, without orientation uncertainties.
The thrust vector $\boldsymbol{T}$ generated by solar sail-based spacecraft is expressed as follows.

$$\boldsymbol{T} = \frac{2P_{\oplus}A}{\rho_{\odot}^2} \times \frac{\hat{\rho}_{\odot}.\hat{\boldsymbol{n}}}{b_1 + b_2 + b_3}\left[b_1\hat{\rho}_{\odot} + \left[b_2(\hat{\rho}_{\odot}.\hat{\boldsymbol{n}}) + b_3\right]\hat{\boldsymbol{n}}\right] \tag{4}$$

$P_{\oplus} = 4.563\mu Pa$ is the solar radiation pressure at Sun-[Earth+Moon] distance, A is the sail reflective area, and $\hat{\boldsymbol{n}}$ is the unit vector normal to the sail nominal surface in the direction opposite to the Sun. The dimensionless parameters $\{b_1, b_2, b_3\}$ are related to the optical characteristics of the sail film material.

$$b_1 = \frac{1-\widetilde{r}}{2}, \qquad b_2 = \widetilde{r}s, \qquad b_3 = \frac{B_f\widetilde{r}(1-s)}{2} + \frac{(1-\widetilde{r})(\epsilon_f B_f - \epsilon_b B_b)}{2(\epsilon_f + \epsilon_b)} \tag{5}$$

where $\widetilde{r}$ is the reflectivity coefficient, s is the fraction of specularly reflected photons, B_f or B_b s the front or back non-Lambertian coefficient respectively, and ϵ_f or ϵ_b is the front

or back sail surface emissivity respectively.
NASA recently approximated the optical properties used in the calculation of $\{b_1, b_2, b_3\}$ using experimental observations and numerical simulations conducted during the preliminary phase of the NEA Scout mission, producing the following results.

$$\widetilde{r} = 0.91, \quad s = 0.89, \quad B_f = 0.79, \quad B_b = 0.67, \quad \epsilon_f = 0.025, \quad \epsilon_b = 0.27 \tag{6}$$

Substituting these values in Eq(5), we get

$$b_1 = 0.095, \quad b_2 = 0.8099, \quad b_3 = 0.015 \tag{7}$$

Let β be the solar sail lightness number (ratio of propulsive acceleration generated in a Sun-facing configuration to the Sun's local gravitational attraction at a given heliocentric distance). The Eq(4) can be re-written in terms of propulsive acceleration vector $\boldsymbol{a}$ as follows.

$$\boldsymbol{a} = \beta \frac{1-\mu}{\rho_{\odot}^2} (\hat{\rho}_{\odot}.\hat{\boldsymbol{n}}) \times \frac{1}{b_1 + b_2 + b_3} \left[b_1 \hat{\rho}_{\odot} + \left[b_2 (\hat{\rho}_{\odot}.\hat{\boldsymbol{n}}) + b_3 \right] \hat{\boldsymbol{n}} \right] \tag{8}$$

4.2 Spacecraft Linearized Dynamics

The premise of this report has been to be able to maintain a solar sail-based spacecraft at a collinear L1 - type AEP (Artificial Equilibrium Point). The continuous propulsive acceleration $\boldsymbol{a}$ is used to displace the natural L1(collinear) point towards the Sun, as is depicted in Figure 2.

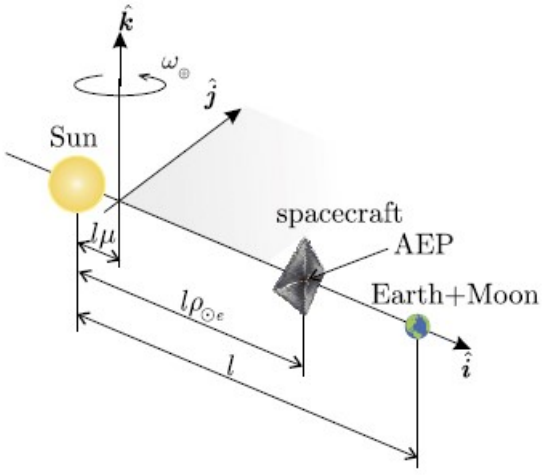

Figure 2: Collinear L1-type AEP

Subscript e is used to denote Sun-sail distance. The location of L1-type AEP can be found by substituting Eq(8) into Eq(3), and by imposing the first and second derivatives of the position vector to be zero. From Fig:2, the dimensionless position and velocity

vectors are,

$$\boldsymbol{r}_e = \left[\rho_{\odot_e} - \mu, 0, 0\right]^T \qquad \dot{\boldsymbol{r}}_e = [0, 0, 0]^T \tag{9}$$

The propulsive acceleration vector $\boldsymbol{a}_e$ is along the $\hat{\boldsymbol{i}}$-direction,

$$\boldsymbol{a}_e = \beta_e \frac{1-\mu}{\rho^2_{\odot_e}} \hat{\boldsymbol{i}} \tag{10}$$

The non-zero component in Eq(3)

$$-\rho_{\odot_e} + \mu + \frac{1-\mu}{\rho^2_{\odot_e}} - \frac{\mu}{(1-\rho_{\odot_e})^2} = \beta_e \frac{1-\mu}{\rho^2_{\odot_e}} \tag{11}$$

$$\beta_e = 1 - \frac{\mu \rho^2_{\odot_e}}{1-\mu} \left[\frac{\rho_{\odot_e}}{\mu} + \frac{1}{(1-\rho^2_{\odot_e})} - 1 \right] \tag{12}$$

To analyse the dynamical behavior of a solar sail-based spacecraft in the vicinity of an L1-type AEP, we use the following transformation

$$\boldsymbol{r} = \boldsymbol{r}_e + \delta\boldsymbol{r} = \left[\rho_{\odot_e} - \mu + x, y, z\right]^T \quad \dot{\boldsymbol{r}} \equiv \delta\dot{\boldsymbol{r}} = [v_x.v_y, v_z]^T \tag{13}$$

$\{x, y, z, v_x, v_y, v_z\} << 1$ are all perturbation terms. Let the state vector $\boldsymbol{x}$ be defined as follows.

$$\boldsymbol{x} = [x, y, z, v_x, v_y, v_z]^T \tag{14}$$

Substituting Eq(13) into Eq(1) and subtracting the equilibrium solution derived in Eq(11), and further neglecting the second-order perturbation terms, we obtain the spacecraft linearized dynamics expression in compact as follows.

$$\dot{\boldsymbol{x}} = \mathbb{A}\boldsymbol{x} \tag{15}$$

$$\mathbb{A} = \begin{bmatrix} \mathbb{O} & \mathbb{I} \\ \mathbb{C} & \mathbb{D} \end{bmatrix} \tag{16}$$

$\mathbb{O}$ is a 3 x 3 zero matrix, $\mathbb{I}$ is a 3 x 3 identity matrix, matrices $\mathbb{C}$ and $\mathbb{D}$ are defined as follows.

$$\mathbb{C} = \begin{bmatrix} c_1 & 0 & 0 \\ 0 & c_2 & 0 \\ 0 & 0 & c_3 \end{bmatrix}, \qquad \mathbb{D} = \begin{bmatrix} 0 & 2 & 0 \\ -2 & 0 & 0 \\ 0 & 0 & 0 \end{bmatrix} \tag{17}$$

$$c_1 = 1 + 2\bar{\mu} - 2\beta_e \frac{1-\mu}{\rho^3_{\odot_e}}, \quad c_2 = 1 - \bar{\mu}, \quad c_3 = -\bar{\mu} \tag{18}$$

$$\bar{\mu} = \frac{\mu}{(1-\rho_{\odot_e})^3} + \frac{1-\mu}{\rho_{\odot_e}^3} \tag{19}$$

Collinear L1-type AEP is unstable, which is demonstrated by the work done in [4]. The matrix $\mathbb{A}$ in Eq(15) has atleast one positive eigenvalue. Hence, in order to be able to maintain AEP, the spacecraft must have a suitable control system.

5 Feedback Control Law

As seen in previous section, a feedback control law for maintenance of equilibrium point is required. Initially, we assumed that the solar sail is capable of modifying both the magnitude and the direction of the propulsive acceleration $\boldsymbol{a}$, and that these modifications can be actuated independently. By varying the direction of the sail normal $\hat{\boldsymbol{n}}$, the direction of the propulsive acceleration vector can be altered.

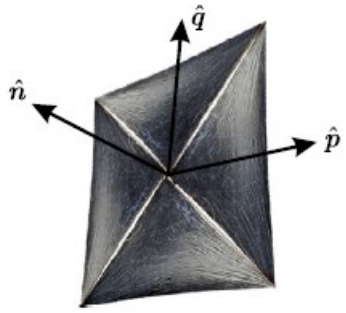

Figure 3: Unit vectors in body-fixed frame $\mathcal{T}_b(S;\hat{\boldsymbol{n}},\hat{\boldsymbol{p}},\hat{\boldsymbol{q}})$

From Eq(8) it is evident that the solar attitude effects the direction of $\boldsymbol{a}$ (through $\hat{\boldsymbol{n}}$). Its is convenient to describe $\hat{\boldsymbol{n}}$ using a body reference frame $\mathcal{T}_b(S;\hat{\boldsymbol{n}},\hat{\boldsymbol{p}},\hat{\boldsymbol{q}})$ with origin at the center of mass of spacecraft S. The unit vectors $\{\hat{\boldsymbol{p}},\hat{\boldsymbol{q}}\}$lie on the sail nominal plane along the principal axes of inertia as shown in Figure 3. $\hat{\boldsymbol{p}}$ lies on the Ecliptic and $\hat{\boldsymbol{q}}$ is perpendicular to it.

All the analysis mentioned till was carried out in Cartesian synodic reference frame $\mathcal{T}(S;\hat{\boldsymbol{i}},\hat{\boldsymbol{j}},\hat{\boldsymbol{k}})$. Two consecutive rotations, of angles θ and ψ, are necessary to superimpose the axes of the synodic reference frame $\mathcal{T}$ to those of the body frame $\mathcal{T}_b$ as depicted below.

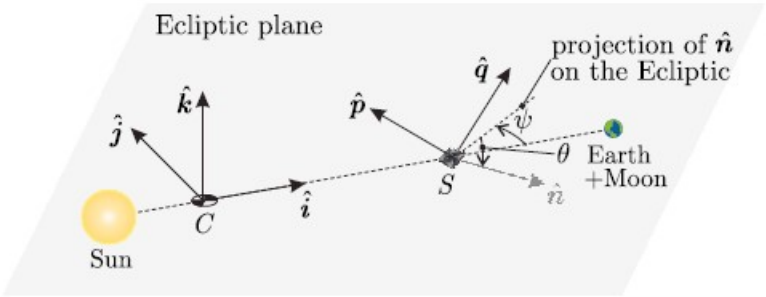

Figure 4: Orientation of $\mathcal{T}$ and $\mathcal{T}_b$

The rotation matrix from $\mathcal{T}$ t $\mathcal{T}_b$ is as follows.

$$\mathbb{R} = \mathbb{R}_2(\theta)\mathbb{R}_3(\psi) = \begin{bmatrix} \cos\theta\cos\psi & \sin\psi\cos\theta & -\sin\theta \\ -\sin\psi & \cos\psi & 0 \\ \cos\psi\sin\theta & \sin\psi\sin\theta & \cos\theta \end{bmatrix} \tag{20}$$

$\mathbb{R}_2$ and $\mathbb{R}_3$ are the principal rotations about the 2- and 3-axis respectively. The third Euler angle would be needed to describe rotation around $\hat{\boldsymbol{n}}$ direction, which however does not affect the orientation of propulsive acceleration vector $\boldsymbol{a}$. Hence its neglected in the analysis. $\hat{\boldsymbol{n}}$ in the synodic frame is

$$[\hat{\boldsymbol{n}}]_{\mathcal{T}} = \mathbb{R}^T \begin{bmatrix} 1 & 0 & 0 \end{bmatrix}^T = \begin{bmatrix} \cos\theta\cos\psi & \sin\psi\cos\theta & -\sin\theta \end{bmatrix}^T \tag{21}$$

Substituting Eq(21) into Eq(8), we obtain the propulsive acceleration in synodic frame $\mathcal{T}$ as follows.

$$[\boldsymbol{a}]_{\mathcal{T}} = \beta\frac{1-\mu}{\rho_{\odot}^2}\cos\psi\cos\theta\frac{1}{b_1+b_2+b_3}\begin{bmatrix} b_1 + b_2\cos^2\psi\cos^2\theta + b_3\cos\psi\cos\theta \\ \cos\theta\sin\psi(b_2\cos\theta\cos\psi + b_3) \\ -\sin\theta(b_2\cos\psi\cos\theta + b_3) \end{bmatrix} \tag{22}$$

We have seen that the sail is in a Sun-facing configuration ($\psi = \theta = 0$ and $\beta = \beta_e$) at the equilibrium condition in L1-type AEP. Therefore, the solar sail is controlled by small variations in lightness number $\delta\beta = \beta - \beta_e$ and through small variations in Euler angles ψ and θ. Hence, the dimensionless control vector is expressed as follows.

$$\boldsymbol{u} = \begin{bmatrix} \delta\beta & \psi & \theta \end{bmatrix}^T \tag{23}$$

Assuming small Euler angles, we have $\cos\psi \simeq 1, \cos\theta \simeq 1, \sin \simeq \psi, \sin\theta \simeq \theta$. Under the

same assumption, the inverse squared Sun-spacecraft distance can be approximated as

$$\rho_{\odot}^{-2} = \left[(\rho_{\odot_e} + x)^2 + y^2 + z^2\right]^{-1} \simeq \rho_{\odot_e}^{-2}(1 - 2x/\rho_{\odot_e})$$

Simplifying the Eq(22) under this assumption of small Euler angles.

$$[\boldsymbol{a}]_{\mathcal{T}} = (\beta_e + \delta\beta)\frac{1-\mu}{\rho_{\odot_e}^2}\left(1 - \frac{2x}{\rho_{\odot_e}}\right)\begin{bmatrix} 1 \\ \psi\frac{b_2+b_3}{b_1+b_2+b_3} \\ -\theta\frac{b_2+b_3}{b_1+b_2+b_3} \end{bmatrix} \tag{24}$$

The minus sign is due to definition of θ (positive when $\hat{\boldsymbol{n}}$ points below Ecliptic).
The linearized spacecraft dynamics expression is obtained by substituting Eq(24) into Eq(1), then subtracting the equilibrium condition in Eq(10). The second order terms are neglected. The resulting dynamical equations are as follows

$$\dot{\boldsymbol{x}} = \mathbb{A}\boldsymbol{x} + \mathbb{B}\boldsymbol{u} \tag{25}$$

$$\mathbb{B} = \begin{bmatrix} \mathbb{O} \\ \mathbb{B}_v \end{bmatrix} \tag{26}$$

$$\mathbb{B}_v = \frac{1-\mu}{\rho_{\odot_e}^2}\begin{bmatrix} 1 & 0 & 0 \\ 0 & \beta\frac{b_2+b_3}{b_1+b_2+b_3} & 0 \\ 0 & 0 & \beta\frac{b_2+b_3}{b_1+b_2+b_3} \end{bmatrix} \tag{27}$$

5.1 Closed-Loop System Dynamics

Full-state feedback control law

$$\boldsymbol{u} = -\mathbb{K}\boldsymbol{x} \equiv -\begin{bmatrix} \mathbb{K}_p & \mathbb{K}_d \end{bmatrix}\boldsymbol{x} \tag{28}$$

$\mathbb{K}_p$ and $\mathbb{K}_d$ are 3x3 matrices of control gains associated with position and velocity components of the state vector $\boldsymbol{x}$. The control gains are selected by means of linear-quadratic regulator(LQR) approach. According to this, the control law minimizes the function

$$J = \frac{1}{2}\int_0^{\infty}(\boldsymbol{x}^T\mathbb{Q}_x\boldsymbol{x} + \boldsymbol{u}^T\mathbb{Q}_u\boldsymbol{u})\mathrm{d}t \tag{29}$$

$\mathbb{Q}_x \geq 0$ and $\mathbb{Q}_u > 0$ are suitable weighting matrices associated with state and control variables respectively. The solution of this LQR problem provides us with $\mathbb{K}$. It is however observed that the off-diagonal terms of $\mathbb{K}_p$ and $\mathbb{K}_d$ are much smaller than the diagonal

elements. Hence, the off-diagonal entries are set to 0.

$$\mathbb{K}_b = \begin{bmatrix} k_{p1} & 0 & 0 \\ 0 & k_{p2} & 0 \\ 0 & 0 & k_{p3} \end{bmatrix} \qquad \mathbb{K}_d = \begin{bmatrix} k_{d1} & 0 & 0 \\ 0 & k_{d2} & 0 \\ 0 & 0 & k_{d3} \end{bmatrix} \tag{30}$$

Here, the gains $\{k_{p1}, k_{d1}\}$ are associated with control variable $\delta\beta$ (hence controls the dynamics along $\hat{\boldsymbol{i}}$ direction), the gains $\{k_{p2}, k_{d2}\}$ are associated with ψ (hence controls the dynamics along $\hat{\boldsymbol{j}}$ direction) and lastly $\{k_{p3}, k_{d3}\}$ aid control in the $\hat{\boldsymbol{k}}$-direction dynamics. Closed-loop system dynamics:

$$\dot{\boldsymbol{x}} = \mathbb{A}\boldsymbol{x} + \mathbb{B}\boldsymbol{u} = \mathbb{A}\boldsymbol{x} - \mathbb{B}\mathbb{K}\boldsymbol{x} = (\mathbb{A} - \mathbb{B}\mathbb{K})\boldsymbol{x} = \widetilde{\mathbb{A}}\boldsymbol{x} \tag{31}$$

The linear stability of the system depends on the eigenvalues of $\widetilde{\mathbb{A}}$ (which is a function of control gains from Eq(31)).

5.2 Control Torques

Control torques are needed to obtain desired θ and ψ. The plan is to estimate the control torques required using Euler equations. To do that the angular velocity ω is written in body-fixed reference frame $\mathcal{T}_b$ with respect to an inertial frame.

$$\omega = \omega_{bs} + \omega_{\oplus} \tag{32}$$

ω_{bs} denotes angular velocity of $\mathcal{T}_b$ wrt synodic reference frame $\mathcal{T}$, $\omega_{\oplus}$ is the angular velocity of $\mathcal{T}$ wrt inertial frame (as seen in Figure 1).

$$\left[\omega_{\oplus}\right]_{\mathcal{T}_b} = \mathbb{R} \begin{bmatrix} 0 \\ 0 \\ \omega_{\oplus} \end{bmatrix} = \begin{bmatrix} -\omega_{\oplus} \sin\theta \\ 0 \\ \omega_{\oplus} \cos\theta \end{bmatrix} \tag{33}$$

$$[\omega_{bs}]_{\mathcal{T}_b} = \dot{\psi}\mathbb{R} \begin{bmatrix} 0 \\ 0 \\ 1 \end{bmatrix} + \dot{\theta} \begin{bmatrix} \cos\theta & 0 & -\sin\theta \\ 0 & 1 & 0 \\ \sin\theta & 0 & \cos\theta \end{bmatrix} \begin{bmatrix} 0 \\ 1 \\ 0 \end{bmatrix} = \begin{bmatrix} -\dot{\psi}\sin\theta \\ \dot{\theta} \\ \dot{\psi}\cos\theta \end{bmatrix} \tag{34}$$

Substituting in Eq(32) and assuming small Euler angles we get,

$$[\omega]_{\mathcal{T}_b} \simeq \begin{bmatrix} -\theta(\dot{\psi} + \omega_{\oplus}) \\ \dot{\theta} \\ \dot{\psi} + \omega_{\oplus} \end{bmatrix} = \begin{bmatrix} \omega_1 \\ \omega_2 \\ \omega_3 \end{bmatrix} \tag{35}$$

$\{\omega_1, \omega_2, \omega_3\}$ are components of ω in body-fixed reference frame $\mathcal{T}_b$.
The sail-attitude controlled dynamics is expressed by the Euler's equations

$$\begin{aligned} I_1\dot{\omega}_1 + (I_3 - I_2)\omega_2\omega_3 &= M_1 \\ I_2\dot{\omega}_2 + (I_1 - I_3)\omega_1\omega_3 &= M_2 \\ I_3\dot{\omega}_3 + (I_2 - I_1)\omega_1\omega_2 &= M_3 \end{aligned} \tag{36}$$

Subscripts 1,2,3 represent the principal axes in the body frame $\mathcal{T}_b$. Substituting Eq(35) in Eq(36),

$$\begin{aligned} M_1 &= -I_1(\ddot{\psi}\theta + \dot{\psi}\dot{\theta} + \omega_{\oplus}\dot{\theta}) + (I_3 - I_2)(\dot{\psi} + \omega_{\oplus})\dot{\theta} \simeq (I_3 - I_1 - I_2)\omega_{\oplus}\dot{\theta} \\ M_2 &= I_2\ddot{\theta} - (I_1 - I_3)(\dot{\psi} + \omega_{\oplus})^2\theta \simeq I_2\ddot{\theta} - (I_1 - I_3)\omega_{\oplus}^2\theta \\ M_3 &= I_3\ddot{\psi} - (I_2 - I_1)(\dot{\psi} + \omega_{\oplus})\dot{\theta}\theta \simeq I_3\ddot{\psi} \end{aligned} \tag{37}$$

Clearly we can observe that the control torques $\{M_1, M_2, M_3\}$ are functions of time histories of the Euler angles. All 3 torques are required to avoid sail-spinning motion.

6 Numerical Simulations

I have done the numerical simulation discussed in [1] using Python. In the process I have used a numerical computing library "Numpy", a scientific computing library "Scipy" and a plotting library called "Matplotlib". I have written the full code in a python notebook. Click the link to access the code.

The time histories of the system state variables are plotted. The given values for this case study are as follows.

$$l\rho_{\odot_e} = 0.988720\text{au}, \qquad \beta_e = 0.0101$$

$$\boldsymbol{x}_0 = \begin{bmatrix} 3.859 \times 10^{-6} & 3.859 \times 10^{-6} & 3.859 \times 10^{-6} & 1.938 \times 10^{-5} & 1.938 \times 10^{-5} & 1.938 \times 10^{-5} \end{bmatrix}$$

$$\mathbb{K}_p = \begin{bmatrix} 22.40 & 0 & 0 \\ 0 & 1.18 \times 10^4 & 0 \\ 0 & 0 & 1.28 \times 10^4 \end{bmatrix}, \quad \mathbb{K}_d = \begin{bmatrix} 7.01 & 0 & 0 \\ 0 & 3.16 \times 10^3 & 0 \\ 0 & 0 & 3.10 \times 10^3 \end{bmatrix} \tag{38}$$

Upon calculation $\widetilde{\mathbb{A}}$ was found to be

$$\widetilde{\mathbb{A}} = \begin{bmatrix} 0 & 0 & 0 & 1 & 0 & 0 \\ 0 & 0 & 0 & 0 & 1 & 0 \\ 0 & 0 & 0 & 0 & 0 & 1 \\ -15.629 & 0 & 0 & -7.171 & 2 & 0 \\ 0 & -111.48 & 0 & -2 & -29.27 & 0 \\ 0 & 0 & -121.742 & 0 & 0 & -28.72 \end{bmatrix}$$

The closed-loop system was found to be stable as all the six eigenvalues of $\widetilde{\mathbb{A}}$ had negative real parts.

$$\lambda_1 = -24.5, \quad \lambda_2 = -23.55, \quad \lambda_3 = -5.47, \quad \lambda_4 = -5.169, \quad \lambda_{5,6} = -3.232 \pm 1.591j$$

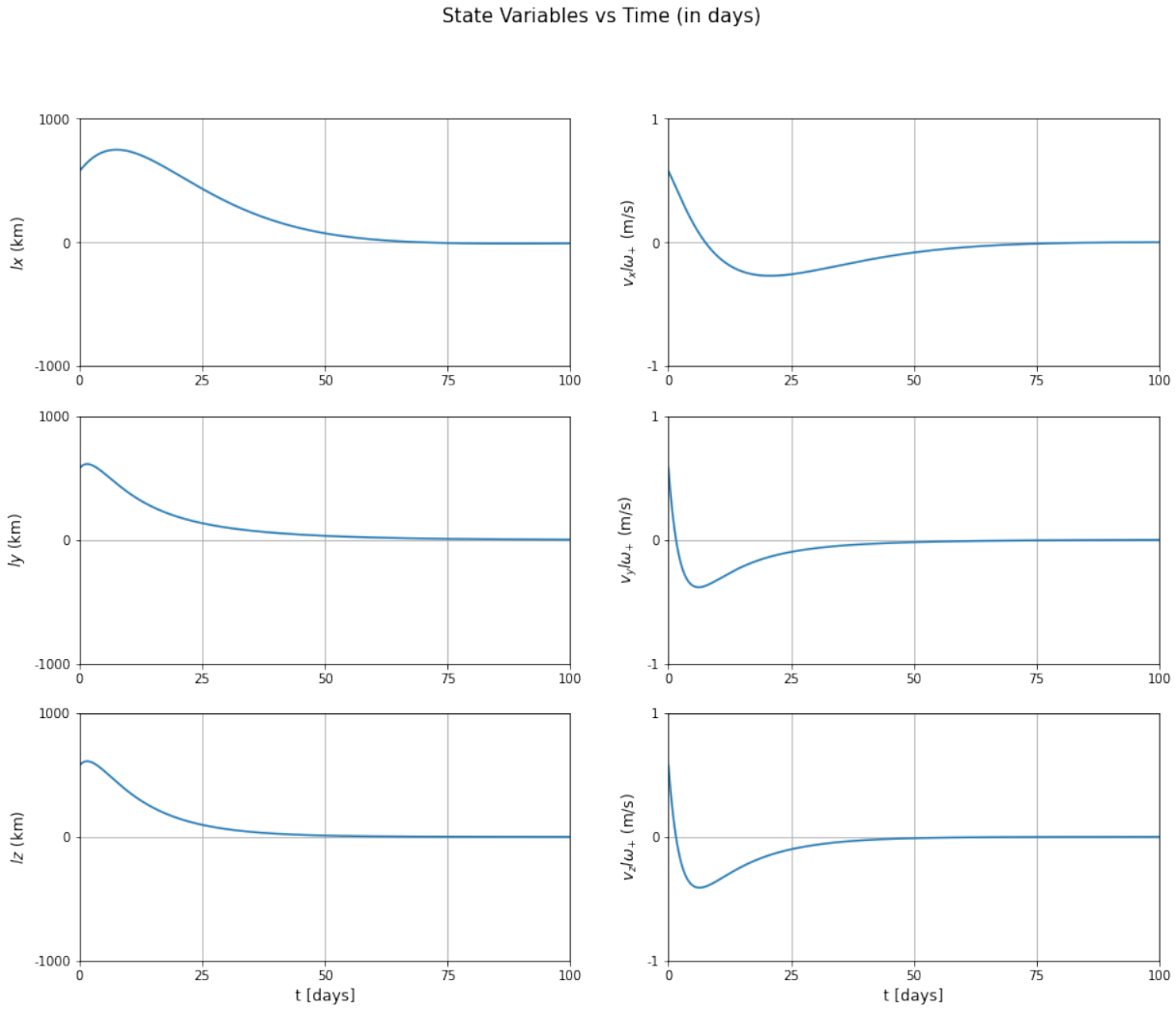

Figure 5: Time Histories of system state variables with gains given by Eq(38)

As a comparative study, the above results are compared with further simplified control

law design. The system dynamics are re-simulated by setting $k_{p2} = k_{p3} = k_{d2} = k_{d3} = 0$. Now, the only effective control variable is $\delta\beta$. The matrix $\widetilde{\mathbb{A}}$

$$\widetilde{\mathbb{A}} = \begin{bmatrix} 0 & 0 & 0 & 1 & 0 & 0 \\ 0 & 0 & 0 & 0 & 1 & 0 \\ 0 & 0 & 0 & 0 & 0 & 1 \\ -15.629 & 0 & 0 & -7.171 & 2 & 0 \\ 0 & -2.153 & 0 & -2 & 0 & 0 \\ 0 & 0 & -3.153 & 0 & 0 & 0 \end{bmatrix} \tag{39}$$

New eigenvalues again indicate system stable

$$\lambda_{1,2} = -3.507 \pm 2.57j, \quad \lambda_{3,4} = -0.078 \pm 1.332j, \quad \lambda_{5,6} = \pm 1.776$$

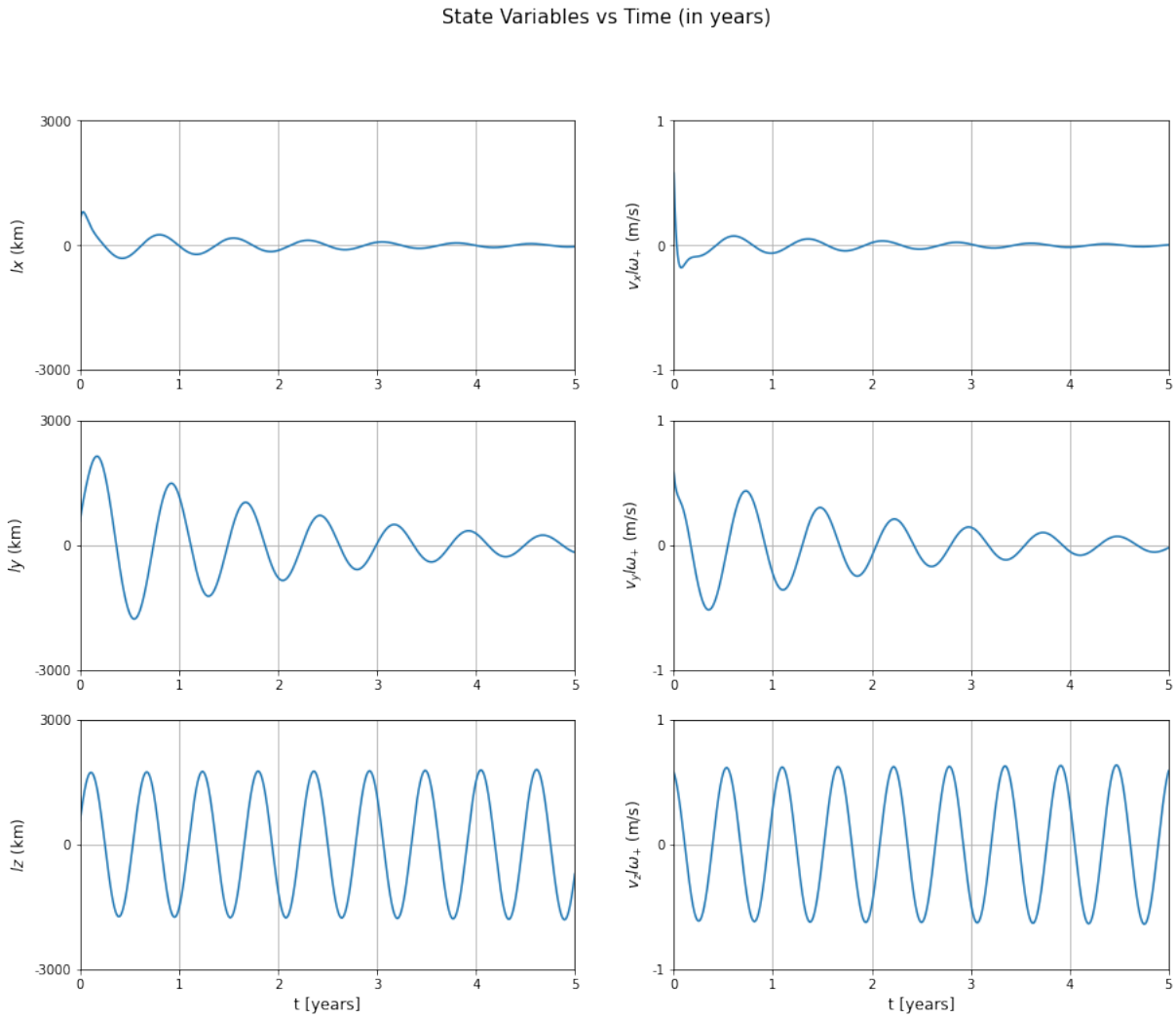

Figure 6: Time Histories of system state variables with simplified control law

The motion on the Ecliptic is stable and the spacecraft moves towards the L1-type AEP

position as shown in the Figure 7 (starting from the red dot to the green dot).

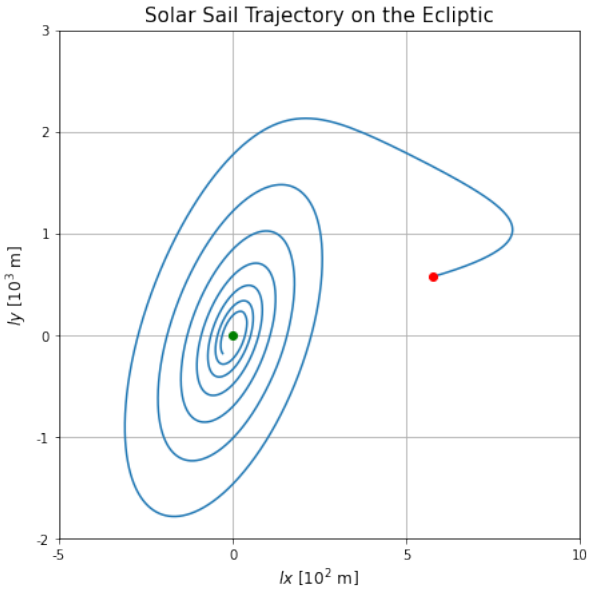

Figure 7: Solar sail trajectory on the Ecliptic relative to L1- type AEP with simplified control law

7 Conclusion

The obtained results through the numerical simulations show that a simplification of the control system is possible, with a negligible decrease of the performance level defined in terms of early warning time for a solar observation mission. From system dynamics perspective, although the spacecraft moves towards the L1-type AEP, the system dynamics with the simplified control law is significantly slower, and the in-plane distance of the spacecraft from the AEP becomes negligible only after a few years. The numerical findings reveal that the mission performance is mostly influenced by dynamics in the radial direction, and that an effective control may be achieved by adjusting the sail lightness number appropriately.

8 Possible Improvements

In the analysis above, the optical force model was used. Although it provides good results, the optical force model happens to neglect certain issues like sail billowing effect, sail film's optical degradation with time, fluctuations of solar radiation pressure and sail film's roughness. So I believe considering a more complex model which takes into account one or more above mentioned issues is one possible way to improve the current analysis.

References

[1] Lorenzo Niccolai, Giovanni Mengali, Alessandro A. Quarta, Andrea Caruso, Feedback control law of solar sail with variable surface reflectivity at Sun-Earth collinear equilibrium points, Aerospace Science and Technology, Volume 106, 2020, 106144, ISSN 1270-9638, https://doi.org/10.1016/j.ast.2020.106144.

[2] Aliasi, G., Mengali, G. Quarta, A.A. Artificial equilibrium points for a generalized sail in the elliptic restricted three-body problem. Celest Mech Dyn Astr 114, 181–200 (2012).https://doi.org/10.1007/s10569-012-9425-z

[3] Koon, W.S., Lo, M.W., Marsden, J.E. and Ross, S.D. (2011) Dynamical Systems: The Three Body Problem and Space Mission Design. Springer, New York, 335 p. http://www.cds.caltech.edu/∼koon/research/3body/Equadiff_mission_2-8-00.pdf

[4] J.D. Biggs, C.R. McInnes, Passive orbit control for space-based geo-engineering, J. Guid. Control Dyn. 33(3) (2010) 1017–1020. http://dx.doi.org/10.2514/1.46054